

1 **On Entrained Pore Size Distribution of Foamed Concrete**

2
3 **Ameer A. Hilal*, Nicholas Howard Thom, Andrew Robert Dawson**

4 *Department of Civil Engineering, Faculty of Engineering, University of Nottingham,*
5 *University Park, Nottingham NG7 2RD, UK Tel: +44 (0) 115 846 8427, Fax: +44 (0) 115*
6 *951 3909, E-mail: evxaah@nottingham.ac.uk*

7 *Corresponding author

8
9 **Abstract**

10 The pore structure of foamed concrete is a significant characteristic since it affects properties
11 such as strength and durability. To investigate these properties, the determination of total air
12 voids content is not sufficient as the shape, size and distribution of air voids may also be
13 influential. To understand the formation of voids after hardening, an investigation of the
14 bubble size distribution of foam (before adding to the mixture) and the pore size distribution
15 of the foamed concrete mixes (after hardening) is discussed in this paper. These distributions
16 have been quantified by examining selected size parameters to make a comparison between
17 them. In addition, void circularity factors have been determined to examine the phenomenon
18 of voids merging. In order to investigate the foam structure before adding to the mix, it was
19 found that by treating the foam with bitumen emulsion, a clear image of its structure can be
20 captured using an optical microscope. Using this technique, a significant difference was
21 found between the size distribution of foam bubbles and those of air pores within foamed
22 concrete mixes. From circularity factor results, there is evidence for increased bubble
23 merging with increased added foam volume (decreased density).

24 **Keywords:** Foamed concrete, Pore structure, Circularity factor, Optical microscope, Image
25 processing.

29 **1. Introduction**

30 Foamed concrete is a versatile material consisting of either Portland cement paste or cement
31 filler matrix (mortar) with homogeneous pore structure created by entrained air voids roughly
32 0.1-1.0 mm size [1-4]. Nambiar and Ramamurthy [1], reported that the introduction of pores
33 inside foamed concrete can be achieved mechanically either by preformed foaming (forming
34 the foam before adding it to the mix) or mix foaming (mixing in a foaming agent). It should
35 be noted that the foamed concrete investigated in this study has been manufactured using the
36 preformed foaming method.

37 The pore structure of cementitious material is a very significant characteristic since it affects
38 properties such as strength and durability due to their dependence on material porosity and
39 permeability [2]. However, determination of the total air void content (porosity) is not
40 sufficient as shape, size and distribution of voids may affect the strength and durability of
41 concrete [5].

42 Ramamurthy et al [2], mentioned that the air-void distribution is one of the most significant
43 micro-properties influencing the strength of foamed concrete and concluded that foamed
44 concrete with a narrower air-void size distribution shows higher strength.

45 It seems likely that the pore structure and microstructure of foamed concrete has an important
46 influence on its properties. It is usually classified into gel pores ($<10\text{nm}$), capillary pores
47 ($<10\mu\text{m}$) and air voids (air entrained and entrapped pores). Although the gel pores do not
48 influence the concrete strength, they are directly related to creep and shrinkage. On the other
49 hand, capillary and other large pores are responsible for reduction in strength and elasticity
50 [1]. In spite of this significant influence, evaluation of foamed concrete pore structure is
51 seldom reported [6].

52 Nambiar and Ramamurthy [1] and Just and Middendorf [7] both mentioned that the pores of
53 foamed concrete can be measured by several test methods such as: nitrogen gas absorption-
54 desorption, optical microscopy with image processing, mercury porosimetry and X ray
55 computed tomography with image processing. In addition, for testing the pore structure and
56 microstructure of foamed concrete, both scanning electron microscopy (SEM) and light
57 microscopy combined with digital imaging were used by Yu et al, [6]. The results from both
58 measurement techniques revealed that the pore diameters were mainly in the range of 100-
59 200 μm .

60 In their investigation into the microstructure of foamed concrete produced with the inclusion
61 of either classified (pfa) and unclassified (Pozz-fill) fly ash, Kearesely [5] concluded that
62 there was no obvious difference between the void sizes observed in the two mixes and that
63 for a 1500 kg/m^3 mix, the entrained air void diameters varied between approximately 40 and
64 $300 \mu\text{m}$.

65 Nambiar and Ramamurthy [1] also determined the air void size distribution of foamed
66 concrete mixes with different added foam volumes (10%, 30% and 50%) and found that the
67 size of the larger voids increased sharply with an increase in foam volume, while for the same
68 foam volume they were smaller for a cement-fly ash mix compared to a cement-sand mix.

69 Thus, although the pore size distribution of foamed concrete has to some extent been
70 investigated, a great deal remains to be understood, so this paper aims to investigate the
71 formation of the voids during mixing. This is achieved by:

- 72 1) Determining and comparing the size distributions of air voids in the foamed concrete
73 mixes (after hardening) to those of bubbles in the preformed foam based on both
74 number and area of bubbles/voids.
- 75 2) Investigating the circularity of the voids within the mixes.

76 **2. Experimental details**

77 **2.1 Constituent materials**

78 The materials used were: ordinary Portland cement CEM I-52,5 N (3.15 S.G.) conforming to
79 BS EN 197-1:2011 [8], natural fine aggregate (sand) (2.65 S.G.) conforming to BS 882:1992
80 [9], sieved to remove particles greater than 2.36 mm to help improve the flow characteristics
81 and stability of the final product [10, 11], potable water and foam. Three mixes of foamed
82 concrete were made with nominal densities of 1300, 1600 and 1900 kg/m^3 , designated FC3,
83 FC6 and FC9. To achieve these target densities, the water cement ratios of these mixes were
84 determined, by trials, ensuring the stability of the wet foamed concrete mix and also that the
85 measured density was equal or nearly equal to the design density [12, 13]. The materials
86 required per m^3 of the selected mixes were calculated using the absolute volume method. An
87 ordinary mixer was used to produce foamed concrete in the laboratory by the addition of
88 preformed foam to a base mortar (sand-cement) mix. The required amount of foam was
89 generated and added to the base mix and mixed until the foam was uniformly distributed and
90 incorporated into the mix [12]. The mix proportions of the foamed concrete mixes
91 investigated are given in **Table 1** per m^3 of final concrete.

92 **2.2 Specimen preparation**

93 - **Foam**

94 Pre-formed foam (at 45 kg/m³) produced by blending a foaming agent, EABASSOC (1.05
95 S.G.), water and compressed air at predetermined proportions of 55: 1 (water: foaming agent
96 by volume) in a foam generator. A STONEFOAM-4 generator was used in this study.

97 About a litre of foam has been taken from the foam generator and then put in a cylindrical
98 plastic container (50mm diameter and 20mm height) for the foam surface microscopic
99 investigation. Due to the impossibility of capturing a clear image of the foam in its natural
100 state using an optical microscope with low magnification, it was decided to impregnate it
101 with a very small dose of bitumen emulsion, see **Figure (1)**. Bitumen emulsion was chosen
102 since it contains carbon which, when using an optical microscope, gives an image with good
103 clarity and contrast between the edges and surfaces of individual foam bubbles, see **Figure**
104 **(2)**. In addition, the production process of bitumen emulsion involves a surfactant (emulsifier)
105 which surrounds individual bitumen droplets (of size <10 µm) within the water, which is
106 essentially the same mechanism as used in foam production, see **Figure (3)**. The result is that
107 the bitumen emulsion will be compatible with the foam and spread easily through the bubble
108 membranes, giving them colour.

109 - **Foamed concrete**

110 For each foamed concrete mix, 3 slices (50 × 50 × 15mm) were cut from the centres of three
111 cured specimens, perpendicular to the cast face, and used for pore size investigation.

112 To make the boundaries between the air voids and the matrix sharp and easily
113 distinguishable, the specimens were first polished and cleaned to remove any residues. Then,
114 to enhance the contrast, the specimen surfaces were treated by applying two coats of
115 permanent marker ink to them. After placing them in an oven at 50°C for 4 hrs, a white
116 powder (Sodium bicarbonate) with a minimum particle size 5 µm was pressed into the
117 surfaces of the specimens and forced into the voids. This left the concrete surface black and
118 the voids white, resulting in specimens with excellent properties for image analysis. This
119 technique is described more fully in EN 480-1 [14] and [1].

120

121

122

123 **2.3 Image capture, processing and analysis**

124 A camera connected to an optical microscope (MCA NIKON SMZ-10 STEREO) and a
125 computer was used to capture the images of both foam and foamed concrete mixes.

126 For the foam investigation, a magnification of (56×) was selected, with a pixel representing
127 2.34 μm and an image of 28.3 mm² (6.14mm × 4.60mm). However, its proved impossible to
128 derive a binary image suitable for automated analysis (in ImageJ) and manual measurements
129 were therefore carried out to determine the void diameters (around 200 voids in each image)
130 from the captured foam images.

131 For mixes, a magnification of (23×) was selected with a pixel representing 6 μm and an
132 image size of 178.52 mm² (15.43mm × 11.57mm). This magnification was chosen in order
133 that air voids with diameters in excess of 20 μm could be easily identified, see Section 3.2.
134 Ten images were captured for each mix and then digitized, converted into binary form and
135 analysed. For this study, only two phases, air voids and solid, were of interest.

136 A histogram of gray levels from the optical microscope image was used to select the
137 threshold value, below which all pixels were considered voids and above which they were
138 considered as solid, creating the final binary image required for analysis. Although the gray-
139 scale histograms did not have a sharp boundary between the two phases (voids and matrix)
140 interface, there was always a minimum in the boundary region and this was set as the
141 threshold for analysis of the images in this study.

142 Although software operations such as dilation, erosion, opening, closing and hole filling have
143 all been suggested as being useful in application to concrete microscopy [1], in this study, it
144 was found that the simple operation of hole filling was sufficient since there is a sharp
145 contrast between the white coloured air voids and the surrounding black coloured matrix.
146 Typical binary images for the three investigated mixes are shown in **Figure (4)**.

147

148

149

150

151

152 3. Results and discussion

153 3.1 Bubble size distribution of foam

154 The bubble size distribution and the corresponding cumulative frequencies (on the basis of
155 number of bubbles) for the foam images are shown in **Figure (5)**. From this, it can be seen
156 that the minimum bubble diameter is about 100 μm and the largest is 875 μm with a median
157 diameter D_{50} of 325 μm and a 90th percentile (D_{90}) of 600 μm . However, it was observed that
158 the natural surface of the foam formed in such a way as to conceal some of the smaller
159 bubbles, and a second set of ten images was therefore captured from the same foam samples
160 after applying a microscope glass slide to the surfaces, see **Figure (6)**. From this figure, the
161 membrane thickness between two bubbles is about 100 μm and since the individual bitumen
162 droplets are less than 10 μm , little effect on the observed bubble diameters is anticipated.

163 The numeric cumulative frequency curves for the foam with and without glass plate
164 application are shown in **Figure (7)**.

165 3.2 Pore size distribution of foamed concrete

166 For each void, an effective diameter was calculated by measuring the void area and assuming
167 it to be perfect circle [5].

168 **Figure (8)** shows the resulting pore size distributions for foamed concrete mixes with
169 densities of 1300, 1600 and 1900 kg/m^3 (mixes FC3, FC6 and FC9 respectively), where it
170 may be seen that sizes vary between approximately 20 and 1950 μm . It is clear that at higher
171 density, the proportion of the larger voids decreases leading to a narrower air void size
172 distribution. In order to quantify and compare the air void distribution of different mixes, the
173 parameters O_{50} (median opening pore size) and O_{90} (90th percentile) were calculated on the
174 basis of number of voids, see Table 2; O_{50} varied from 165 to 180 μm , O_{90} from 525 to 750
175 μm , and both O_{50} and O_{90} increased with foam volume. The smallest air void diameter
176 identified was about 20 μm . To check that these smallest pores came from the added foam
177 (entrained air voids) rather than from the manufacturing process (entrapped air voids), SEM
178 images were captured from mortar mixes both with and without added foam, **Figures (9)** and
179 **(10)**. In **Figure (10)**, it can be seen that there are very few entrapped air voids in the 20 μm
180 size range, leading to the conclusion that all pores in excess of 20 μm , clearly apparent in
181 **Figure (9)**, are foam pores.

182 The calculations were repeated this time by calculating the O50 and O90 on the basis of the
183 area contained within each void (see **Table 2**). This is discussed in the next section.

184

185 **3.3 Comparison**

186 **Figure (8)** illustrates the cumulative frequency of bubble/ pore diameters in the foam and the
187 foamed concrete mixes (on the basis of number of bubbles/voids). Two very clear differences
188 are apparent. First, foamed concrete mixes contain some larger sized pores than those in the
189 foam itself and the number of such pores increasing with the increase in added foam volume.
190 This is logical due to the combining of foam bubbles during and possibly after mixing.
191 However, the second difference is much more substantial. From **Figure (5)**, the smallest
192 bubble diameter in the foam was about 100 μm , while in the foamed concrete mixes there
193 were many voids with sizes lower than this value. Even when microscope glass slide was
194 pressed into the foam surface, **Figure (6)**, no more than 20% of bubbles were found to be
195 smaller than 100 μm (**Figure 7**) and it could be argued that this technique leads to bubble
196 distension and an overestimation of bubble diameters. In contrast, 30-40% of voids in the
197 mixes had a diameter less than 100 μm . Looking at the D_{50} values, that for foam was 300-325
198 μm , depending on the observational technique used, compared to 165-185 μm for the mixes.

199 There are two possible reasons for this. Firstly; merging of large bubbles, by reducing the
200 number of larger voids, reduces the total number of voids compared to that of foam bubble
201 leading to an increase in the numeric proportion of the smallest voids and positioning the
202 numeric cumulative curve for the mix above the curve for the foam.

203 Secondly, from a vacuum saturation test; it was found that the porosities of the mortars
204 (without foam) are 14.6, 14.1 and 13.9% for FC3, FC6 and FC9 respectively. While for the
205 FC3, FC6 and FC9 foamed concrete, they were 52.8, 40.9 and 29%. By knowing the added
206 foam (**Table 1**) and the difference between foamed concrete and corresponding mortar
207 porosities, it was found that there is foam volume loss of about 4.2, 2.7 and 1.5% for FC3,
208 FC6 and FC9 respectively. This loss is probably because foam bubbles collapse or the air in
209 them is lost to the atmosphere, and this is likely happening with the large bubbles. This will
210 have the same effect of merging leading to the median diameter of foam bubbles (D_{50}) being
211 larger than those of the voids (O_{50}) in the mixes.

212 Another possible interpretation is that the loss of foam bubbles (by collapse) during the
213 mixing process leaves a solution (foaming agent with water) which works as an air-entraining

214 agent and produces, during mixing, other smaller bubbles. In this context, the addition of a
215 foam stabilizer could usefully be investigated and the bubble size distribution in the hardened
216 concrete examined.

217 In place of analysis of numbers of bubbles at each diameter, the same data was considered
218 from the prospective of the area of the bubbles in the foam and the concrete images. **Figure**
219 **(11)** shows the frequency and cumulative frequency by area of the bubbles in the foam. This
220 may be contrasted with the numeric frequency previously presented in Figure (5). A low
221 number of larger bubbles (**Figure 5**) means that the area contained within these bubbles
222 comprises a significant proportion of the space occupied by the foam, as seen in **Figure (11)**
223 between 550 and 875 μm . This has the effect of increasing the D_{50} calculated on the basis
224 area (470 μm) from the value of 325 μm calculated on the basis of number of bubbles (**Table**
225 **2**). Because in concrete the larger bubbles are more implicated in the development of
226 cracking and, hence, strength reduction, the characterisation by bubble area is probably to be
227 preferred. Continuing this argument, characterization by, for example, D_{90} may be more
228 germane.

229 A comparison of foam bubble area and concrete mix pore area is included in **Table 2**. It
230 shows that both median and large characteristic voids are significantly greater in area than in
231 the foam. This implies that there has been significant merging of small voids into a few larger
232 voids during the concrete mixing process. This behaviour is most pronounced in the least
233 dense mix.

234 Considering this observation with the early one that median pore size based on number of
235 pores reduces, comparison of **Figures (8)** and **(12)** allows us to deduce that bubble merging is
236 prevalent in all mixes. In the less dense mixes, bubble merging takes place at all sizes (the
237 cumulative area void curve for the concrete is always beneath that for the foam). In the most
238 dense mix the area contained in small pores does not change much at all, indicating that the
239 small bubbles result in small pores without much loss to merged bubbles.

240 In the most dense mix, since the voids merging of larger voids is less than in the lighter
241 mixes, loss of voids must be more effective than their merging in making the mix curve lie
242 above the foam curve within the small diameter range (**Figure 12**).

243 Considering all the foamed concretes in **Figure (12)**, the small or absence of curve increase
244 in the small diameter range indicates that bubble splitting/shrinkage does not occur in any
245 mixes or if it does, bubble merging offsets its effect.

246 **3.4 Pore Circularity**

247 The circularity factor (F_{circ}) is the function of a perimeter and surface area of each pore,
248 defined as follows;

$$249 \quad F_{circ} = 4\pi \left[\frac{Area}{perimeter^2} \right] \quad (1)$$

250 Circularity factor equals 1 for a perfect circular pore and it is smaller for irregular shapes
251 [15].

252 From the SEM images for foamed concrete mixes (Figure (8)), it can be seen that the voids
253 shape, at high magnification ($> 500\times$), is almost circular which means that their circularity
254 factor should be near to 1. However, with the optical microscope (at low magnification,
255 $< 25\times$); voids with irregular shapes, formed due to bubble merging, can clearly be seen; see
256 Figure (4) supported by lower magnification SEM images in **Figure (13)**. From image
257 analysing results, **Figure (14)** shows that void merging is more frequent with decreased
258 added foam volume. Therefore, the F_{circ50} and F_{circ90} for FC9 are higher than those of FC3; see
259 cumulative frequency curves in **Figure (14)** and **Table (2)**. This effect, bubble merging, is
260 likely to be a primary reason that the porosity values (36.6, 25 and 14 for FC3, FC6 and FC9
261 respectively) calculated by image analysis were lower than the added foam volumes (42.4,
262 29.5 and 16.6), a reason also suggested by Nambiar and Ramamurthy [1], and the difference
263 increases with increased added foam (decrease in density).

264

265

266

267

268

269

270

271 **4. Conclusion**

272 From the tests presented in this paper and based on the above results and discussion, the
273 following conclusions can be drawn:

- 274 - By treating with bitumen emulsion, a clear image, of foam bubbles shape and
275 distribution, can be captured using an optical microscope.
- 276 - There is a difference between the size distribution of bubbles within preformed foam
277 and those of pores in foamed concrete mixes.
- 278 - Compared to the foam bubble size distribution, some larger sized pores were
279 presented in foamed concrete mixes owing to the merging of bubbles during mixing.
- 280 - Bubble merging in all mixes is relatively significant, the greater merging being
281 observed in the lowest density mixes, but only larger bubbles appear to participate in
282 their merging.
- 283 - All foamed concrete mixes investigated also contained a higher proportion of small-
284 sized voids compared to the preformed foam, meaning that the D_{50} of the foam was
285 larger than that of all investigated mixes. This is likely due to merging and losing of
286 bubbles during mixing.
- 287 - Bubble splitting or shrinkage does not appear to be significant in any mix or if it does,
288 bubble merging and loss offsets its effect.
- 289 - For foamed concrete mixes (on the basis of number or area of voids), O_{50} and O_{90}
290 both decrease with decreased added foam volume (increase in density).
- 291 - Although both in the foam and in the concrete mixes made with the foam the median
292 (D_{50}) bubble/void is relatively small when the overall number of bubbles is
293 monitored, yet there are a small number of larger bubbles/voids which, by virtue of
294 their size, contribute a significant proportion of the area (and hence volume) of voids
295 in the concrete mixes. Because larger voids are more implicated in concrete weakness,
296 it is recommended that definition of voids on the basis of area is to be preferred.
- 297 - From circularity factor results, the evidence for bubbles merging is higher with
298 increased added foam volume (decrease in density).

299 This study has suggested a number of avenues for future research including:

- 300 - Using different doses of the bitumen emulsion and investigating their effect on the
301 observed bubbles thickness.
- 302 - Addition of foam stabilizer and its effect on bubble size distribution in hardened
303 concrete.

304 **Acknowledgements**

305 The authors would like to acknowledge the support of the Higher Committee for
306 Education Development in Iraq (HCED) for the research scholarship enabling this work
307 to be conducted as part of a larger research project. The authors also wish to thank Dr
308 Daniel Wells (E-A-B Associates Company, UK) for providing the foaming agent. Finally,
309 the valuable help and comments of Mr Keith Dinsdale (University of Nottingham) during
310 the microscopy observation and Mr Martin Roe (University of Nottingham) during the
311 SEM test are gratefully acknowledged.

312

313

314

Table 1. Mix proportions of selected foamed concrete mixes.

	Mixes		
	FC3	FC6	FC9
Target density (kg/m ³)	1300	1600	1900
Cement content (kg/m ³)	500	500	500
W/C ratio	0.475	0.5	0.525
Water content (kg/m ³)	237.5	249.9	262.5
Sand content (kg/m ³)	562	850	1137.5
Foam (l/m ³)	424	295	166
Foaming agent (kg/m ³)	0.35	0.24	0.14

315

316

317

318

319

320

321

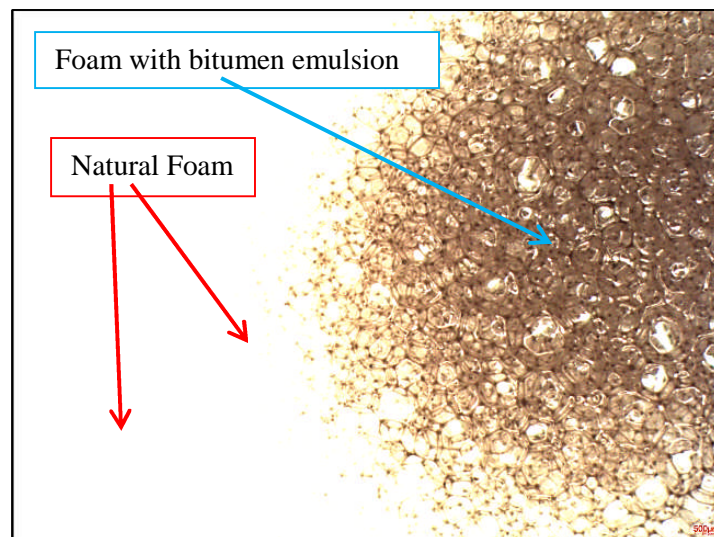
322

323

324

325

326



327

Fig. 1. Image of foam during bitumen emulsion application.

328

329
330
331
332
333
334
335
336
337
338

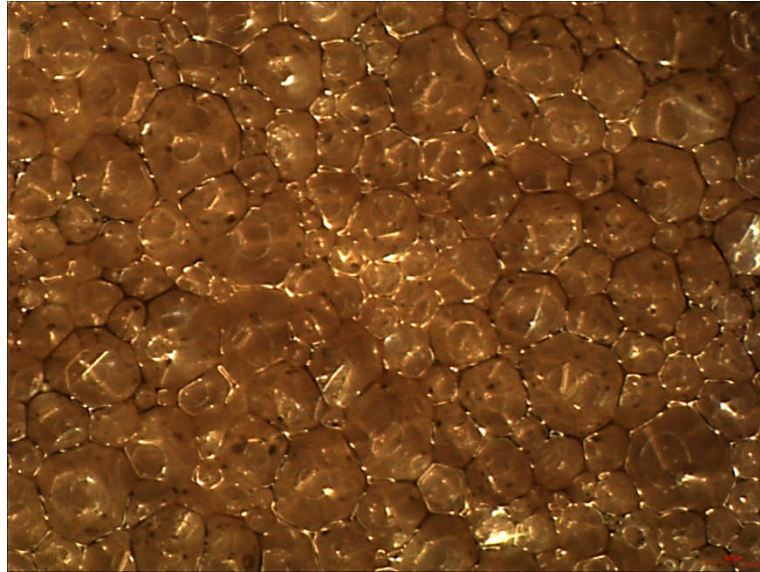


Fig. 2. Foam after treating with bitumen emulsion.

339
340
341
342
343
344
345
346
347
348
349

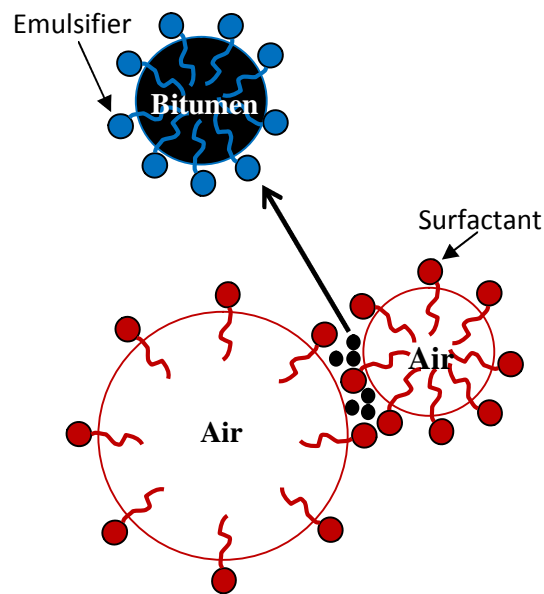


Fig. 3. The interaction between foam bubbles and bitumen emulsion.

351
352
353
354
355
356
357

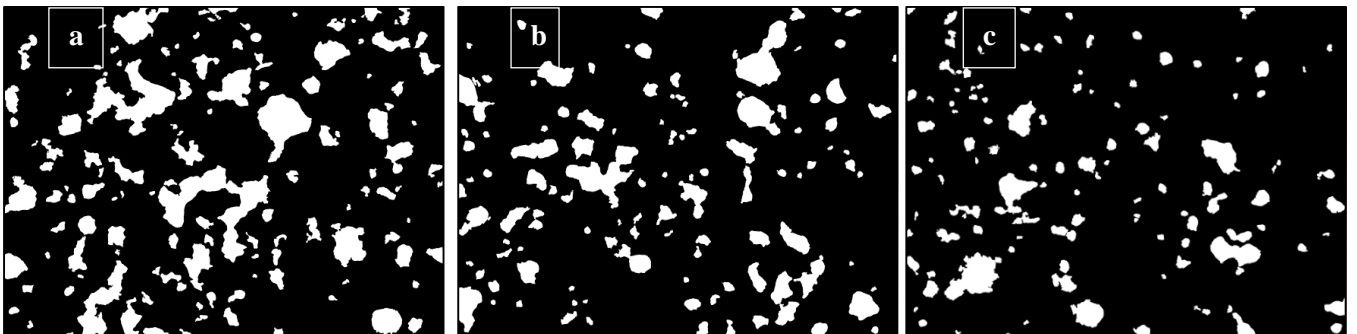
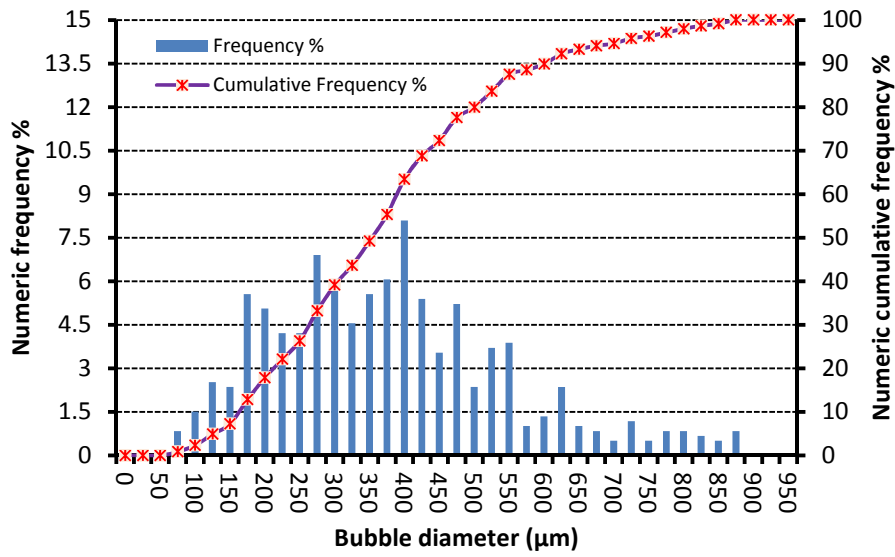


Fig. 4. Typical binary images [15.43mm × 11.57mm] a) FC3, b) FC6 and c) FC9.

358

359



360

361

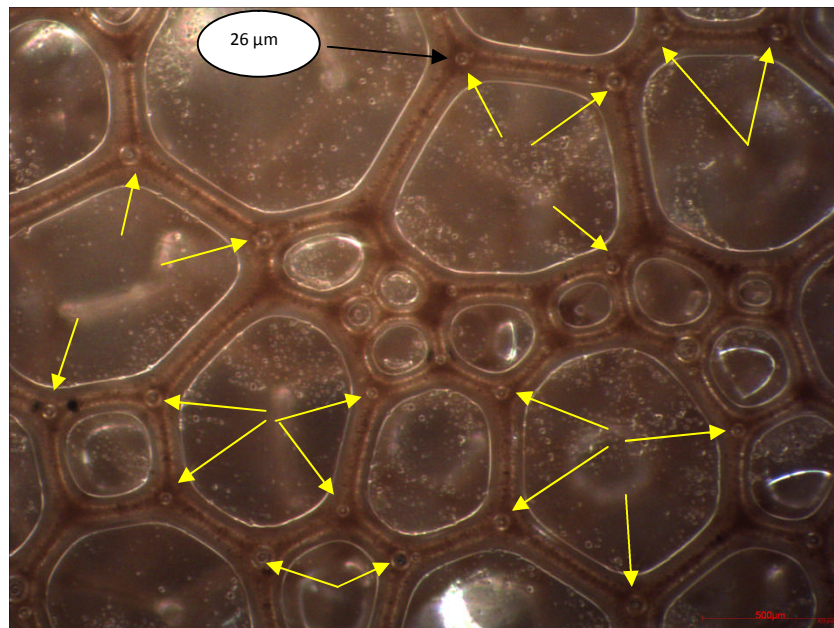
362

Fig. 5. Numeric bubble size distribution and cumulative frequency of foam.

363

364

365



366

367

368

369

370

371

372

373

374

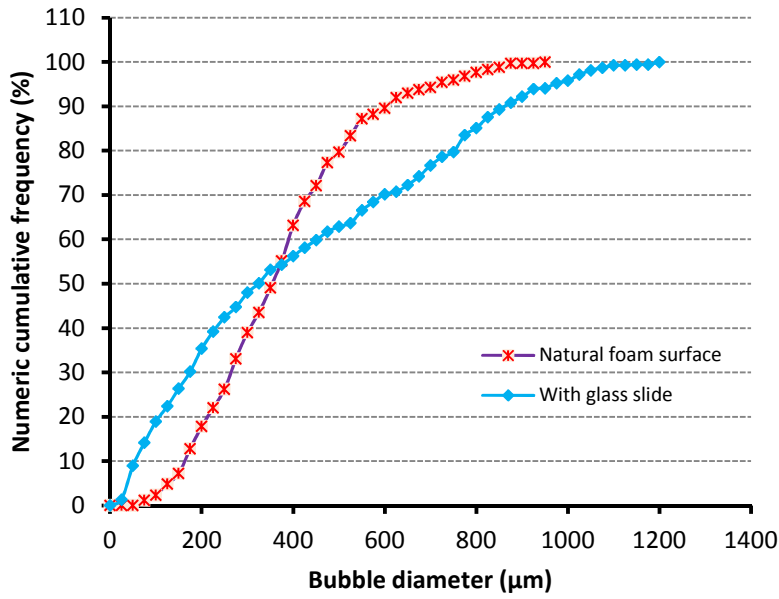
375

Fig. 6. Foam image showing voids with diameters less than 100 µm by applying a microscope glass slide to the foam surface.

376

377

378



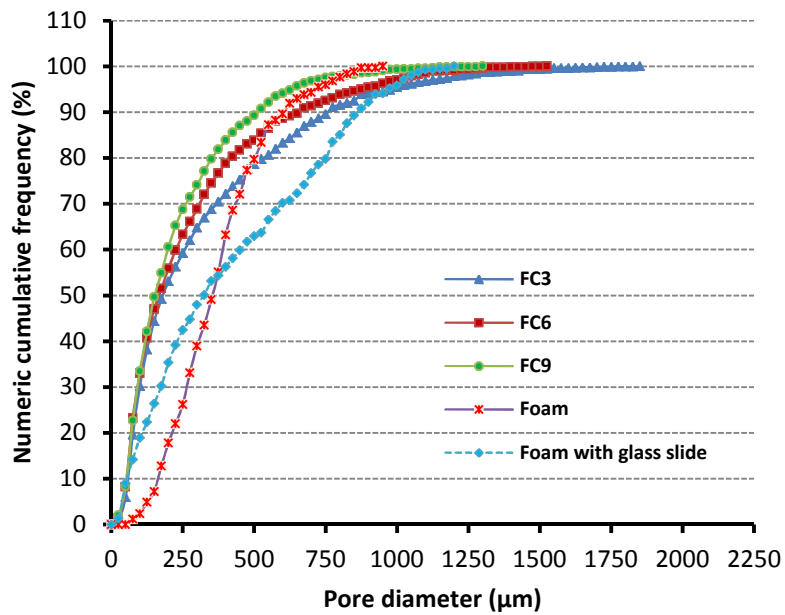
379

380 Fig. 7. Numeric cumulative frequency of foam with and without glass slide application.

381

382

383



384

385 Fig. 8. Numeric cumulative frequency of bubble/pore diameters of foam and foamed concrete mixes.

386

387

388

389 Table 2. Parameters of pores sizes and circularity of foam and mixes.

	Foam	FC3	FC6	FC9
(D or O) ₅₀ * (μm)	325	180	175	165
(D or O) ₉₀ * (μm)	600	750	650	525
(D or O) ₅₀ ** (μm)	470	770	685	550
(D or O) ₉₀ ** (μm)	765	1425	1225	990
F _{circ50}		0.53	0.59	0.65
F _{circ90}		0.75	0.80	0.84

390 Note: Diameter of bubbles (D) and voids (O) derived either from cumulative distribution based on numeric of
 391 bubbles/voids^(*) at each size or on area of bubbles/voids^(**) at each size.

392

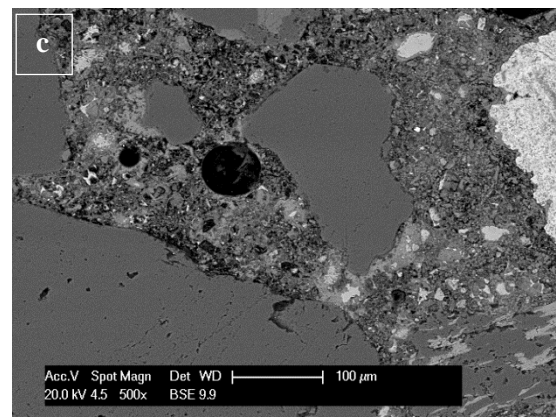
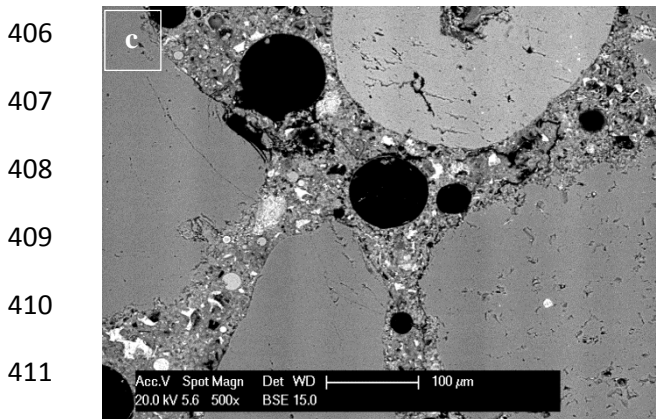
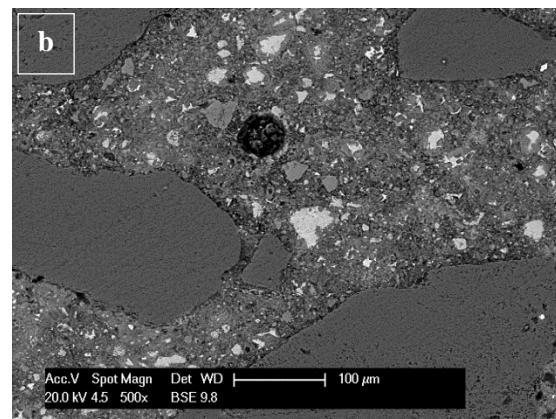
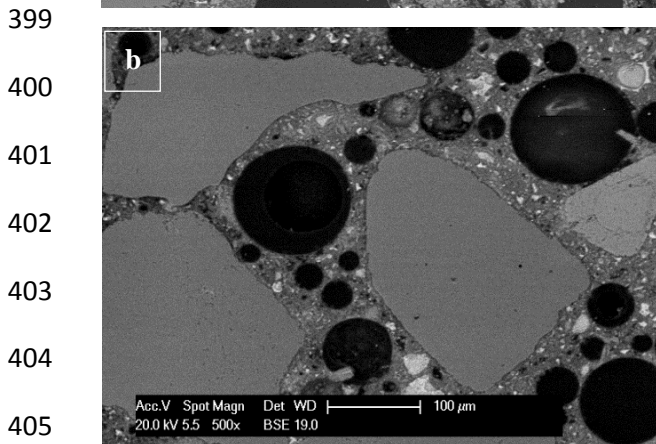
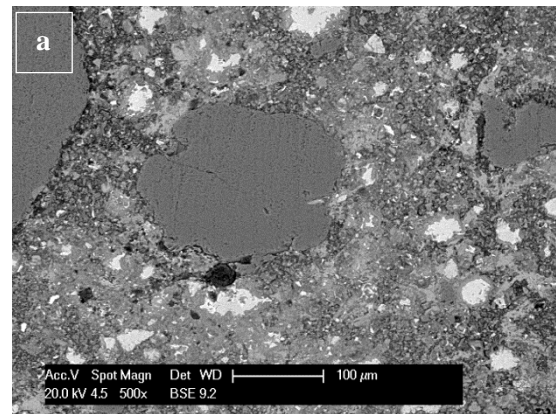
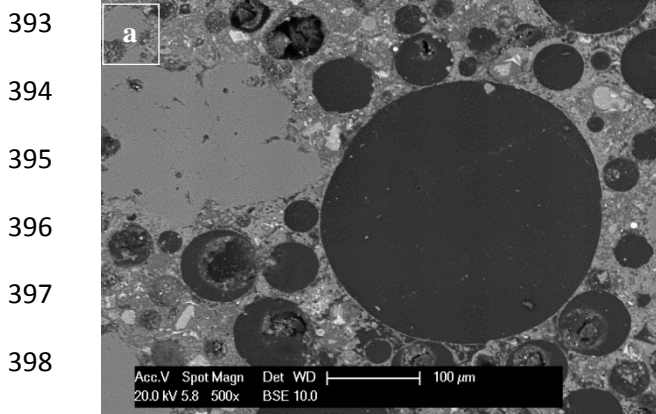
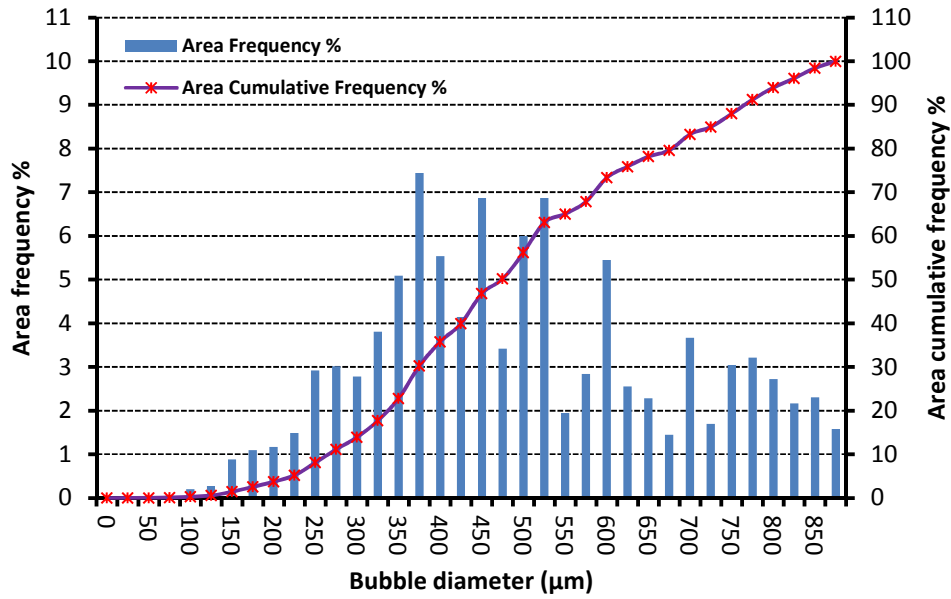


Fig. 9. SEM images of foamed concrete mixes
 a) FC3, b) FC6 and c) FC9.

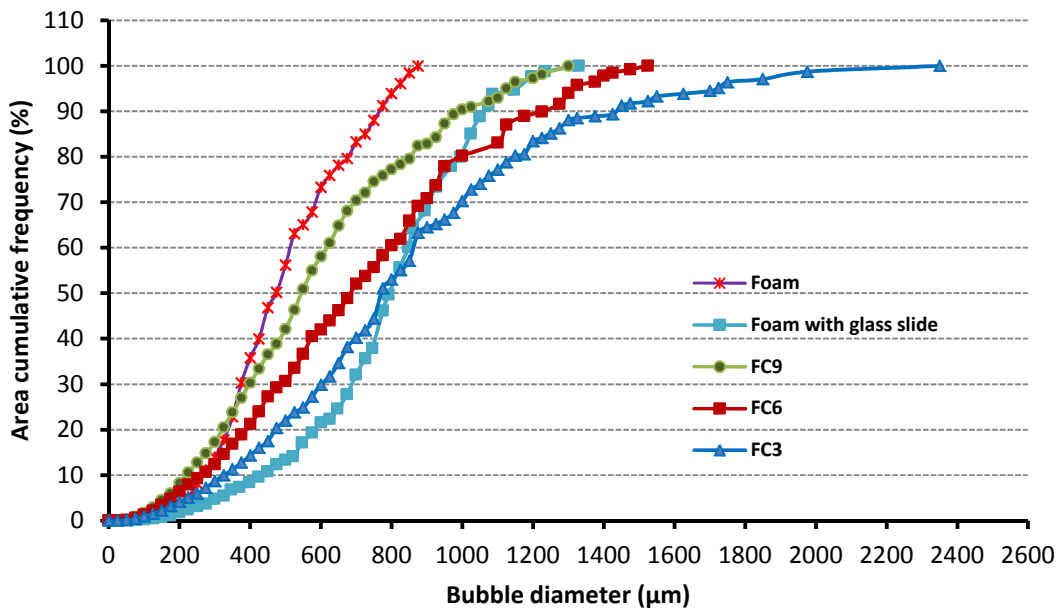
Fig. 10. SEM images for mixes without foam
 a) 1300 b) 1600 and c) 1900 kg/m³.



413

414

Fig. 11. Area bubble size distribution and cumulative frequency of foam.



415

416

Fig. 12. Area cumulative frequency of bubble/pore diameters of foam and foamed concrete mixes.

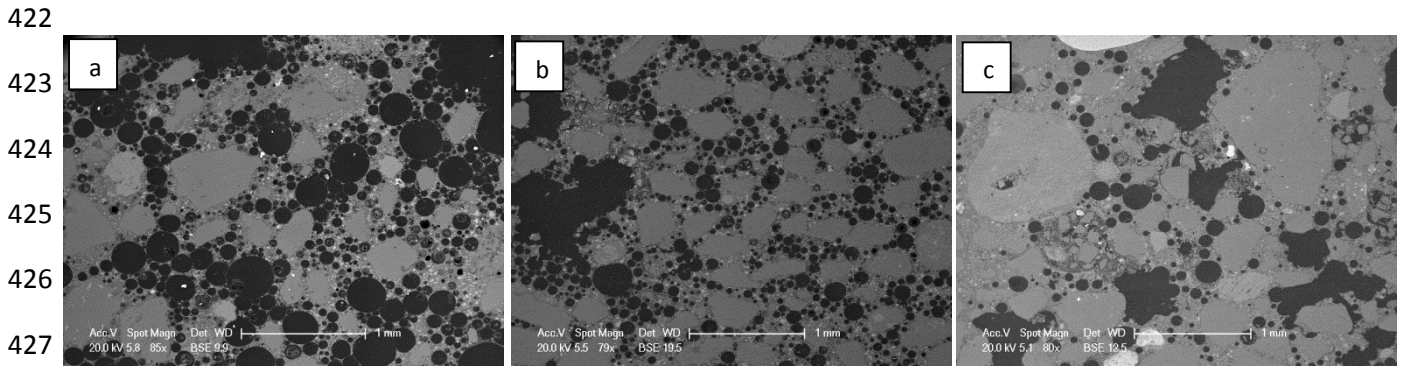
417

418

419

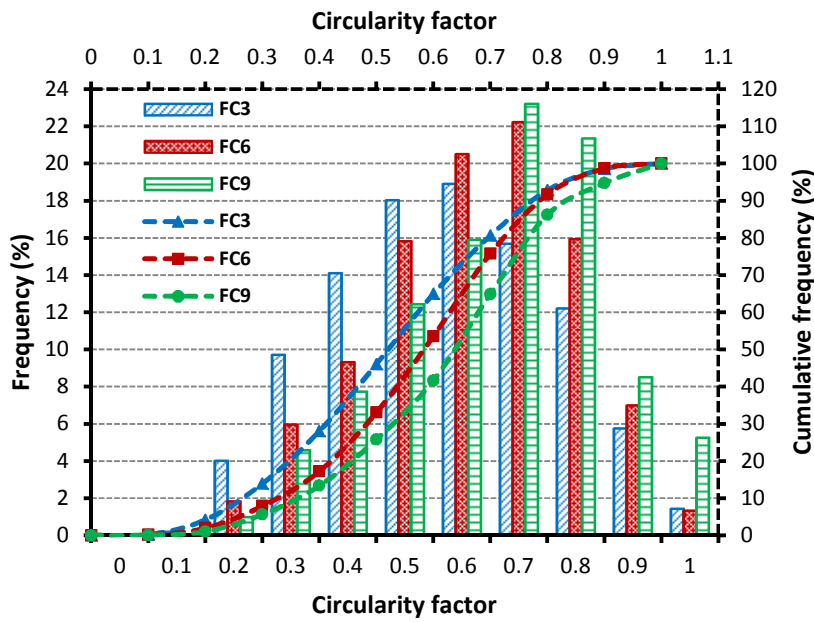
420

421



428 Fig. 13. SEM images of foamed concrete mixes showing the bubble merging a) FC3, b) FC6 and c)
429 FC9.

430
431
432



433
434
435
436
437
438
439
440
441

Fig. 14. Circularity factor of foamed concrete mixes.

442 **References**

- 443 1. Nambiar, E. and K. Ramamurthy, *Air-void characterisation of foam concrete*. Cement and
444 concrete research, 2007. **37**(2): p. 221-230.
- 445 2. Ramamurthy, K., E.K. Kunhanandan Nambiar, and G. Indu Siva Ranjani, *A classification of*
446 *studies on properties of foam concrete*. Cement and Concrete Composites, 2009. **31**(6): p.
447 388-396.
- 448 3. Othuman, M.A. and Y.C. Wang, *Elevated-temperature thermal properties of lightweight*
449 *foamed concrete*. Construction and Building Materials, 2011. **25**(2): p. 705-716.
- 450 4. Jitchaiyaphum, K., T. Sinsiri, and P. Chindaprasirt, *Cellular Lightweight Concrete Containing*
451 *Pozzolan Materials*. Procedia Engineering, 2011. **14**(0): p. 1157-1164.
- 452 5. Kearsley, E., *The Effect of High Volume of Ungraded Fly Ash on the Properties of Foamed*
453 *Concrete*, in *School of Civil Engineering 1999*, The University of Leeds: Leeds.
- 454 6. Yu, X.G., et al., *Pore Structure and Microstructure of Foam Concrete*. Advanced Materials
455 Research, 2011. **177**: p. 530-532.
- 456 7. Just, A. and B. Middendorf, *Microstructure of high-strength foam concrete*. Materials
457 Characterization, 2009. **60**(7): p. 741-748.
- 458 8. BS EN 197-1, *Cement-Part 1: Composition, Specifications and Conformity Criteria for*
459 *Common Cements*, in *British Standards Institution, London*. 2011.
- 460 9. BS 882, *Specification for aggregates from natural sources for concrete*. British Standards
461 Institution, London, 1992.
- 462 10. ASTM C144, *Standard Specification for Aggregate for Masonry Mortar*. 1987, American
463 Society for Testing and Materials.
- 464 11. Jones, M. and A. McCarthy, *Preliminary views on the potential of foamed concrete as a*
465 *structural material*. Magazine of concrete research, 2005. **57**(1): p. 21-31.
- 466 12. Nambiar, E.K.K. and K. Ramamurthy, *Sorption characteristics of foam concrete*. Cement and
467 concrete research, 2007. **37**(9): p. 1341-1347.
- 468 13. Nambiar, E.K.K. and K. Ramamurthy, *Fresh state characteristics of foam concrete*. Journal of
469 materials in civil engineering, 2008. **20**: p. 111.
- 470 14. BS EN 480-11, *Admixtures for concrete, mortar and grout- Test methods- Part 11:*
471 *Determination of air void characteristics in hardened concrete*. 2005: British Standards
472 Institution, London.
- 473 15. Scheffler, M. and P. Colombo, *Cellular ceramics: structure, manufacturing, properties and*
474 *applications*. 2005: WILEY-VCH Verlag GmbH & Co. KGaA.

475

476

477

478

479

480

481

482

483

484

485 **Figures Captions**

- 486 Fig. 1. Image of foam during bitumen emulsion application.
- 487 Fig. 2. Foam after treating with bitumen emulsion.
- 488 Fig. 3. The interaction between foam bubbles and bitumen emulsion.
- 489 Fig. 4. Typical binary images [15.43mm × 11.57mm] a) FC3, b) FC6 and c) FC9.
- 490 Fig. 5. Numeric bubble size distribution and cumulative frequency of foam.
- 491 Fig. 16. Foam image showing voids with diameters less than 100 μm by applying a microscope glass
492 slide to the foam surface.
- 493 Fig. 7. Numeric cumulative frequency of foam with and without glass slide application.
- 494 Fig. 8. Numeric cumulative frequency of bubble/pore diameters of foam and foamed concrete mixes.
- 495 Fig. 9. SEM images of foamed concrete mixes a) FC3, b) FC6 and c) FC9.
- 496 Fig. 10. SEM images for mixes without foam a) 1300 b) 1600 and c) 1900 kg/m³.
- 497 Fig. 11. Area bubble size distribution and cumulative frequency of foam.
- 498 Fig. 12. Area cumulative frequency of bubble/pore diameters of foam and foamed concrete mixes.
- 499 Fig. 13. SEM images of foamed concrete mixes showing the bubble merging a) FC3, b) FC6 and c)
500 FC9.
- 501 Fig. 14. Circularity factor of foamed concrete mixes.
- 502
- 503